www.nature.com/aps

Acta Pharmacologica Sinica

ARTICLE

Oridonin ameliorates inflammation-induced bone loss in mice via suppressing DC-STAMP expression

Bin-hua Zou[1,2], Yan-hui Tan[1,2], Wen-de Deng[1,2], Jie-huang Zheng[1,2], Qin Yang[1,2], Min-hong Ke[1,2], Zong-bao Ding[1,2] and Xiao-juan Li[1,2]

Currently, dendritic cell-specific transmembrane protein (DC-STAMP), a multipass transmembrane protein, is considered as the master regulator of cell–cell fusion, which underlies the formation of functional multinucleated osteoclasts. Thus, DC-STAMP has become a promising target for osteoclast-associated osteolytic diseases. In this study, we investigated the effects of oridonin (ORI), a natural tetracyclic diterpenoid compound isolated from the traditional Chinese herb *Rabdosia rubescens*, on osteoclastogenesis in vivo and ex vivo. ICR mice were injected with LPS (5 mg/kg, ip, on day 0 and day 4) to induce inflammatory bone destruction. Administration of ORI (2, 10 mg·kg^{-1}·d^{-1}, ig, for 8 days) dose dependently ameliorated inflammatory bone destruction and dramatically decreased DC-STAMP protein expression in BMMs isolated from LPS-treated mice. Treatment of preosteoclast RAW264.7 cells with ORI (0.78–3.125 μM) dose dependently inhibited both mRNA and protein levels of DC-STAMP, and suppressed the following activation of NFATc1 during osteoclastogenesis. Knockdown of DC-STAMP in RAW264.7 cells abolished the inhibitory effects of ORI on RANKL-induced NFATc1 activity and osteoclast formation. In conclusion, we show for the first time that ORI effectively attenuates inflammation-induced bone loss by suppressing DC-STAMP expression, suggesting that ORI is a potential agent against inflammatory bone diseases.

Keywords: DC-STAMP; osteoclast; oridonin; NFATc1; inflammatory bone loss

Acta Pharmacologica Sinica (2021) 42:744–754; https://doi.org/10.1038/s41401-020-0477-4

INTRODUCTION

Osteoclasts are multinucleated cells derived from the same lineage of monocyte progenitor cells as dendritic cells (DCs) and macrophages and are responsible for dissolving the organic and mineral components of bone [1, 2]. Classically, osteoclastogenesis is initiated when RANKL binds to its cognate receptor RANK; this process activates multiple signaling pathways that ultimately lead to the induction and nuclear translocation of c-Fos and NFATc1, thus stimulating osteoclast formation and bone resorption by increasing the expression of osteoclast genes, including cathepsin K and TRAP [3–6]. Through enhanced bone resorption activity, overactivated osteoclasts play a key role in bone loss diseases, which affect hundreds of millions of people [7–10]. Inhibition of osteoclast differentiation has become a new therapeutic strategy for bone diseases, including rheumatoid arthritis, osteoporosis, and metastatic cancer [9, 11, 12].

DC-specific transmembrane protein (DC-STAMP), a multipass transmembrane protein, is currently considered a master regulator of osteoclastogenesis [12–14]. DC-STAMP is indispensable for the fusion of osteoclastic precursor cells and the formation of multinucleated mature osteoclasts [12, 14, 15]. During RANKL-induced osteoclast differentiation, DC-STAMP expression is increased in osteoclast precursors [16, 17]. DC-STAMP deficiency completely abrogated the fusion of macrophages to form multinucleated mature osteoclasts, even when cells were cultured at densities that allowed migration-independent cell–cell contact [13, 18]. DC-STAMP-knockout mice had few multinucleated osteoclasts and increased bone density [19]. Conversely, DC-STAMP Tg mice had an increased number of osteoclasts and bone loss [20]. In addition, knocking out DC-STAMP reduced NFATc1 protein expression during osteoclastogenesis, and the decreased NFATc1 expression in DC-STAMP$^{-/-}$ cells was restored by DC-STAMP overexpression [19]. A DC-STAMP antibody inhibited fusion and osteoclast differentiation in both murine and human precursors in vitro and reduced bacteria-induced periodontal bone destruction in vivo [21]. The frequency of circulating DC-STAMP^{+} cells was recently reported to be elevated in inflammatory bone destruction diseases such as psoriatic arthritis [22]. Therefore, DC-STAMP is a therapeutic target for the treatment of osteoclast-associated osteolytic diseases.

Oridonin (ORI) is a plant-derived natural tetracyclic diterpenoid compound isolated from *Rabdosiarubescens*, a traditional Chinese medicinal herb that has therapeutic effects on inflammatory disorders [23] and various cancers, such as colon cancer [24], melanoma [25], lymphoma [26], breast cancer [27], osteosarcoma [28], and leukemia [29]. Recently, ORI has been reported to inhibit ifrd-1- and IκBα-mediated NF-κB translocation to suppress RANKL-induced osteoclastogenesis of bone marrow-derived macrophages (BMMs) and RAW264.7 cells in vitro and ovariectomy-induced osteoporosis in vivo. The mRNA and cytoplasmic c-Fos and NFATc1 expression downstream of NF-κB in BMMs were also reduced by ORI in vitro [30]. Increasing evidence shows that

[1]Laboratory of Anti-inflammatory and Immunomodulatory Pharmacology, School of Pharmaceutical Sciences, Southern Medical University, Guangzhou 510515, China and [2]Guangdong Provincial Key Laboratory of New Drug Screening, School of Pharmaceutical Sciences, Southern Medical University, Guangzhou 510515, China
Correspondence: Xiao-juan Li (lixiaoj@smu.edu.cn)

Received: 13 March 2020 Accepted: 6 July 2020
Published online: 4 August 2020

overactivated osteoclasts participate in inflammatory osteolytic diseases, including rheumatoid arthritis, psoriatic arthritis, and osteoarthritis, which affect hundreds of millions of individuals around worldwide [31]. Notably, while ORI exhibits efficacy in treating inflammatory diseases in animals safely [32], the role of ORI in inflammatory bone loss is not yet known.

Here, we demonstrated a novel mechanism by which ORI inhibited osteoclastogenesis in vitro and ex vivo by suppressing DC-STAMP expression and subsequent NFATc1 activation. Our data also revealed that ORI protected against inflammation-induced bone loss in vivo.

MATERIALS AND METHODS

Reagents

ORI (PubChem CID: 34057) (purity > 98%) was purchased from Chengdumust (Sichuan, China). LPS (055:B5), a leukocyte acid phosphatase (TRAP) kit, and cyclosporin A (CsA) (PubChem CID:5284373) [33] were obtained from Sigma (St Louis, MO, USA). RAW264.7 cells that were stably transfected with NFAT-luciferase were generated as previously described [34]. α-MEM and Australia fetal bovine serum (FBS) were obtained from Gibco (Rockville, MD, USA). Soluble mouse RANKL and soluble recombinant mouse M-CSF were provided by R&D (R&D Systems, Minneapolis, MN, USA). A total isolation mini kit and SYBR Premix Ex Taq were obtained from Promega (Madison, WI, USA). A PrimeScript RT reagent kit was provided by TaKaRa (Dalian, China). A nuclear extraction kit was provided by Wanleishengwu (Wanleibio, Shenyang, China). NFATc1 (D15F1) mAb, β-actin mAb, c-Fos (9F6) mAb, and lamin A/C (4C11) mAb were provided by Cell Signaling Technology (Beverly, MA, USA). PLCγ1 (1249) and p-PLCγ1 (Tyr 783) were provided by Santa Cruz Biotechnology (Santa Cruz, CA, USA). An anti-DC-STAMP mAb (OM203458) was provided by OmnimAbs (CA, USA).

Animal experiments and BMMs preparation

Six-to-eight-week-old female C57BL/6 mice and ICR mice were provided by the Guangdong Medical Laboratory Animal Center (Guangdong, China). The animal protocols were approved by the Institutional Animal Care and Use Committee of Southern Medical University (animal ethics ID: L2015075). BMMs were freshly isolated from bone marrow as previously described [33]. The ICR mice were used for the in vivo experiments.

In vitro osteoclastogenesis assay

RAW264.7 cells and BMMs were obtained and maintained as previously described [33]. The cells were collected and seeded into a 96-well plate at 1×10^3/well or 2×10^4/well and cultured in DMEM with 10% FBS and 100 ng/mL RANKL or in α-MEM supplemented with 30 ng/mL M-CSF, 100 ng/mL RANKL, and 10% FBS with or without different concentrations of ORI (0.39–3.125 μM) at 37 °C in 5% CO_2. After 4–5 days, the cells were stained for TRAP using the leukocyte TRAP kit.

In vitro cell viability assay

The cytotoxic effects of ORI were determined using an MTT assay [33]. Briefly, RAW264.7 cells were seeded in 96-well plates and cultured in complete medium with or without different concentrations of ORI (0.39–3.125 μM) for 8 h, 24 h or 7 days. MTT solution (0.5 mg/mL) was added during the last 4 h of incubation. The optical density was measured at a wavelength of 570 nm using a 96-well microplate reader (Tecan, Austria). Cell viability was expressed as a percentage of the medium control.

Bone absorption assay

RAW264.7 cells and BMMs were seeded in hydroxyapatite-coated plates (Corning, Lowell, MA, USA) at densities of 1×10^3 cells per well and 2×10^4 cells per well, respectively, and cultured in DMEM with 10% FBS and 100 ng/mL RANKL or in α-MEM supplemented with FBS, 100 ng/mL RANKL, and 20 ng/mL M-CSF with or without different concentrations of ORI (0.39–3.125 μM) at 37 °C, 5% CO_2. The medium was changed on day 3. Seven days later, the cells were treated with a 10% bleach solution. Total resorption pits were captured using a light microscope (IX71; Olympus). Pit areas were quantified by Image-Pro Plus 6 software.

RNA extraction and quantitative PCR analysis

Quantitative PCR was used to measure specific gene expression during osteoclast formation. RAW264.7 cells (1×10^6 cells/well) were seeded, treated with ORI for 2 h, and then stimulated with RANKL (100 ng/mL) for 24 h. Total RNA was extracted using an RNeasy mini kit (Promega, Madison, WI, USA). The cDNA was synthesized from 1 μg of total RNA using reverse transcriptase (TaKaRa Biotechnology, Otsu, Japan). Real-time PCR was performed using SYBR Premix Ex Taq™ II (Tli RNase H Plus) (Promega, Madison, WI, USA) and detected using an ABI 7500 sequencing detection system (Applied Biosystems, Foster City, CA, USA). PCR amplification was performed as previously described [33]. The primer sequences of osteoclast-related genes were as follows [33]: OSCAR-F: 5′-CTG CTG GTA ACG GAT CAG CTC CCC AGA-3′, OSCAR-R: 5′-CCA AGG AGC CAG AAA AAC T-3′; c-Fos-F: 5′-CCA GTC AAG AGC ATC AGC AA-3′, c-Fos-R: 5′-AAG TAG TGC AGC CCG GAG TA-3′; DC-STAMP-F: 5′-TGA AAC TAC GTG GAG AGA AGC AA-3′, DC-STAMP-R: 5′-CAG ACA CAC TGA GAC GTG GT-3′; and Fra-2-F: 5′-ATC CAC GCT CAC ATC CCT AC-3′, Fra-2-R: 5′-GTT TCT CTC CCT CCG GAT TC-3′. Values were normalized to the mean expression of GAPDH.

Western blot analysis

RAW264.7 cells (1×10^6 cells/well) were seeded in six-well plates. After treatment with ORI (0.39–3.125 μM) for 2 h, the cells were stimulated with 100 ng/mL RANKL for 30 min or 24 h. Total protein was prepared with RIPA lysis buffer (Fdbio Science, Hangzhou, China), nuclear and cytosolic extracts were generated according to the protocol of the nuclear extraction kit (Wanleibio, Shenyang, China), and protein concentrations were determined using a BCA kit (BCA, Thermo Fisher, MA, USA). Next, 20–30 μg of each protein lysate was separated by 10% sodium dodecylsulfate-polyacrylamide gel electrophoresis (SDS-PAGE, Sigma-Aldrich, St Louis, MO, USA) and transferred to PVDF membranes (Millipore, Bedford, MA, USA). The membranes were blocked in 5% nonfat milk, blotted with the indicated primary antibodies at 4 °C and then incubated with secondary antibodies. Finally, the protein bands were detected using an ECL system (Yeasen Biotech, Shanghai, China) and a multifunctional imaging analysis system (Protein Simple, CA, USA), and the obtained images were analyzed with ImageJ software.

Luciferase reporter gene assays for NFATc1

The effects of ORI on the RANKL-induced NFATc1-luciferase reporter gene were determined as previously described [34]. Briefly, RAW264.7 cells were stably transfected with NFAT-luciferase and seeded in 96-well plates overnight. The cells were then pretreated with ORI or CsA (1 μM) for 30 min, followed by RANKL stimulation for 24 h. NFAT luciferase activity was measured using a luciferase assay system (Promega, Madison, WI, USA).

Knockdown of DC-STAMP by small interfering RNA (siRNA)

RAW264.7 cells were transfected with 40 nM DC-STAMP siRNA (GenePharma Co., Ltd., 199 Dongping Street, Suzhou, China) using Lipofectamine RNAIMAX (Invitrogen) according to the manufacturer's instructions. The RNA oligo sequences were as follows: DC-STAMP-siRNA-1 (sense: 5′-CCA GUG GAU UUA CGG CCU UTT-3′; antisense: 5′-AAG GCC GUA AAU CCA CUG GTT-3′), DC-STAMP-siRNA-2 (sense: 5′-GCU CAU AUG AAU GAC ACU ATT-3′; antisense: 5′-UAG UGU CAU UCA UAU GAG CTT-3′), DC-STAMP-siRNA-3

(sense: 5′-CCA UGA UUC UGC CUU UAA UTT-3′; antisense: 5′-AUU AAA GGC AGA AUC AUG GTT-3′), DC-STAMP-siRNA-4 (sense: 5′-CCC UGC AAA UGA AGA UGA UTT-3′; antisense: 5′-AUC AUC UUC AUU UGC AGG GTT-3′), GAPDH-siRNA (sense: 5′-CAC UCA AGA UUG UCA GCA ATT-3′; antisense: 5′-UUG CUG ACA AUC UUG AGU GAG-3′), and negative control siRNA (sense: 5′-UUC UCC GAA CGU GUC ACG UTT-3′; antisense: 5′-ACG UGA CAC GUU CGG AGA ATT-3′). Two days after transfection, mRNA or protein was isolated and analyzed to determine the transfection efficiency. For TRAP staining after interference, RAW264.7 cells were collected, seeded into 24-well plates at 2×10^4/well, and cultured in DMEM with 10% FBS. After 24 h of siRNA interference, the media were changed, and RANKL (100 ng/mL) with or without different concentrations of ORI (0.39–3.125 μM) was added. The media were changed every 2 days. After 4–5 days, the cells were stained using the TRAP assay kit. NFAT-luc RAW264.7 cells were transfected with DC-STAMP siRNA for 24 h and stimulated with RANKL for 24 h; then, luciferase activity was measured to evaluate NFATc1 transcriptional activity.

Effects of ORI on LPS-induced osteolysis in vivo

We examined the protective effect of ORI on inflammation-induced bone loss in an LPS-induced mouse model [35–38]. Six-week-old female ICR mice were divided into four groups ($n = 7$): PBS treatment (control); LPS injection (LPS); LPS plus 2 mg/kg ORI treatment (LPS + Ori2 mg/kg); and LPS plus 10 mg/kg ORI treatment (LPS + Ori10 mg/kg). The mice received intraperitoneal injections of LPS (5 mg/kg body weight) on days 0 and 4 to induce inflammatory bone destruction. The 2 and 10 mg/kg ORI groups received intragastric administration every day starting on the day before the first LPS injection. All mice were sacrificed on day 7 after the initial injection of LPS. BMMs in the left tibia and femur of each animal were flushed with α-MEM and used for TRAP staining, bone resorption pit assays, and mRNA and protein extraction. The right femur of each animal was scanned using high-resolution microcomputed tomography (micro-CT) (CT80, Scanco Medical, Zurich, Switzerland) with the following instrument parameters: 50 kV, 500 μA, and 0.7° rotation step. After scanning, the right femurs were fixed and decalcified for H&E staining to examine the level of bone erosion and count the number of osteoclasts. Bone histomorphometric analyses were performed using the micro-CT data, and section images were analyzed using a SkyScan™ CT analyzer and light microscope; the numbers of osteoclasts per bone surface were quantified with Image-Pro Plus software.

Statistical analysis

All experiments, except the in vivo mouse studies, were performed at least three times. One-way ANOVA, followed by Dunnett's multiple comparison post hoc test, was used to determine differences between different groups. A value of $P < 0.05$ was considered a statistically significant difference.

RESULTS

ORI ameliorated inflammation-induced bone loss in vivo

The protective effect of ORI against LPS-induced bone loss was first examined. The micro-CT results and 3D reconstruction images showed that LPS induced extensive bone loss in the mouse femurs (Fig. 1a–c). In addition, the BMD, BV/TV, and Tb.N in the LPS treatment group were markedly decreased in comparison with those parameters in the PBS treatment group, whereas the Tb.Sp was increased in LPS-treated mice. Compared with the LPS group, the groups treated with 2 and 10 mg/kg ORI exhibited notable increases in BMD, Tb.N, and BV/TV, as well as markedly reduced Tb.Sp (Fig. 1c, d). Furthermore, histological examination confirmed that ORI treatment prevented LPS-induced bone destruction (Fig. 1e). Dramatic inflammatory bone erosion was observed in the LPS group, while ORI treatment considerably blocked inflammatory bone erosion, as shown by H&E staining (Fig. 1e). Collectively, these data demonstrated that ORI prevented LPS-induced osteolysis in vivo.

ORI decreased DC-STAMP protein expression in vivo

To further reveal the intrinsic mechanism by which ORI slows LPS-induced bone destruction in vivo, we determined the mRNA expression of osteoclast-specific genes, such as TRAP and OSCAR, in BMMs from the model and ORI-treated groups. The results showed that 2 and 10 mg/kg ORI treatment decreased the mRNA levels of OSCAR and TRAP compared with those of the model condition, indicating that ORI may have an inhibitory effect on osteoclast formation in LPS-induced osteolysis in vivo (Fig. 1f, g). In addition, we found that 2 and 10 mg/kg ORI treatment dramatically downregulated DC-STAMP protein expression in BMMs from LPS-injected model mice (Fig. 1h, i). Collectively, these results suggest that ORI prevents LPS-induced osteolysis in vivo by inhibiting osteoclastogenesis and downregulating DC-STAMP expression.

ORI decreased osteoclast formation and osteoclast resorption in BMMs ex vivo and RANKL-induced osteoclastogenesis in RAW264.7 cells in vitro

BMMs from inflammatory model mice and ORI-treated mice were obtained and differentiated into osteoclasts with 20 ng/mL RANKL for 3 or 7 days for TRAP and pit assays, respectively. The BMMs from LPS-injected model mice showed dramatically increased $TRAP^+$ osteoclast formation and bone resorption activity compared with those of control mice. Moreover, BMMs from 2 and 10 mg/kg ORI-treated mice had markedly reduced osteoclast formation, as shown by the TRAP assay, and reduced resorption functions, according to the osteoclastic pit assay, compared with those of model mice. BMMs are precursor cells of osteoclasts in mice, and these results further demonstrated that ORI reduced osteoclastogenesis to attenuate inflammatory bone destruction in vivo (Fig. 2a–c).

As typical osteoclast precursors, RAW264.7 cells form TRAP-positive multinucleated osteoclasts and resorb bone in the presence of RANKL [39]. Consistent with a previous report [30], we observed that ORI at concentrations of 0.39–3.125 μM suppressed osteoclast formation and bone resorption without cytotoxicity (Fig. 2d–g). Therefore, ORI inhibited RANKL-induced osteoclast formation and resorption in RAW264.7 cells beginning at a concentration of 0.39 μM in vitro.

ORI inhibited DC-STAMP expression during osteoclastogenesis in RAW264.7 cells in vitro

DC-STAMP is necessary for the fusion of precursor cells to form mature and functional osteoclasts, and the expression of DC-STAMP was upregulated in RAW264.7 cells stimulated with RANKL [16]. Our results showed that pretreatment with 1.56 or 3.25 μM ORI inhibited RANKL-induced mRNA and protein expression of DC-STAMP (Fig. 3a–c).

ORI suppressed c-Fos and NFATc1 activation in RAW264.7 cells in vitro

DC-STAMP can mediate osteoclastogenesis by promoting the expression of c-Fos and NFATc1 [19, 39, 40]. DC-STAMP deficiency decreases NFATc1 expression [19]. The RANKL-induced increases in c-Fos mRNA and total protein levels in RAW264.7 cells were abrogated upon treatment with 0.78, 1.56, or 3.125 μM ORI (Fig. 4a–c). Furthermore, ORI dramatically decreased the nuclear translocation of c-Fos during RANKL-induced osteoclastogenesis (Fig. 4d, e).

In addition, RANKL-upregulated NFAT-luciferase activity was dose dependently suppressed by ORI and 1 μM CsA (Fig. 5a). NFATc1 mRNA and total protein levels and nuclear translocation

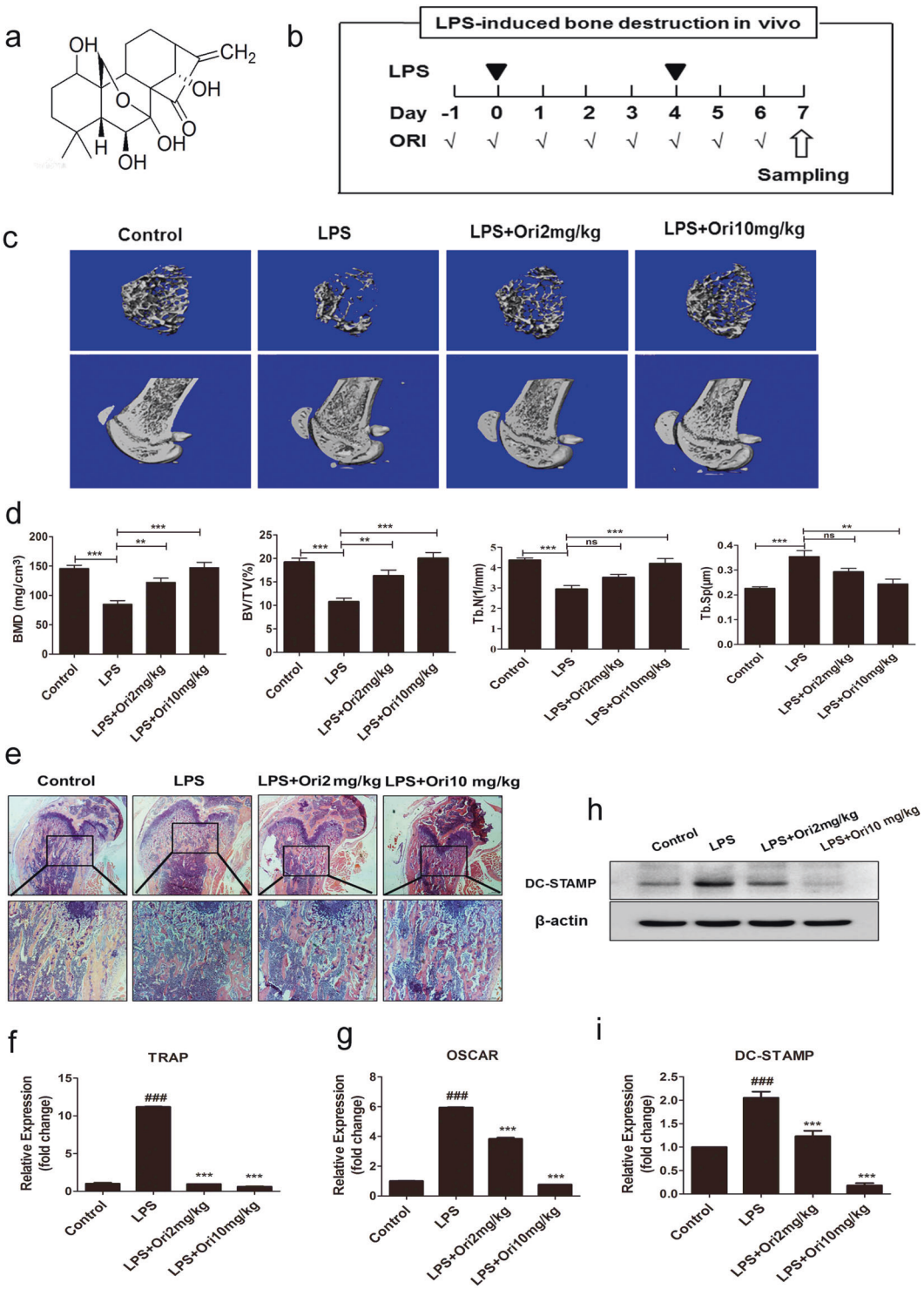

Fig. 1 ORI ameliorated inflammation-induced bone loss and DC-STAMP in vivo. a Molecular structure of oridonin (ORI). **b** Mice were intraperitoneally injected with LPS (5 mg/kg) or PBS at 0 and 4 days. ORI (2 and 10 mg/kg) was administered intragastrically daily for 8 days. **c** Representative 3D micro-CT reconstructed images of trabecular bone from the femurs of mice in each group (control group, LPS group, and LPS group treated with 2 or 10 mg/kg ORI) ($n = 7$). **d** The microstructural parameters, including Tb.N, Tb.Sp, BMD, and BV/TV. **e** The right femurs were fixed and stained with H&E. The BMMs from the left tibias and femurs of mice in each group were collected to measure the mRNA expression of **f** TRAP and **g** OSCAR and **h**, **i** the protein expression of DC-STAMP. The results are presented as the mean ± SD of representative experiments. $^{###}P < 0.001$ vs the control group; $^{**}P < 0.01$, $^{***}P < 0.001$ vs the LPS group.

were also blocked upon treatment with 0.78, 1.56, or 3.125 μM ORI (Fig. 5b–f). PLCγ1 is related to Ca^{2+} signaling, which is upstream of NFATc1 activation [33]. Treatment with 0.78–3.125 μM ORI for 30 min reduced the RANKL-induced phosphorylation of PLCγ1 (Fig. 5g, h). These data indicated that ORI could inhibit c-Fos and NFATc1 activation in RAW264.7 cells during RANKL-induced osteoclasts formation, which was consistent with the reduced osteoclastogenesis and DC-STAMP results.

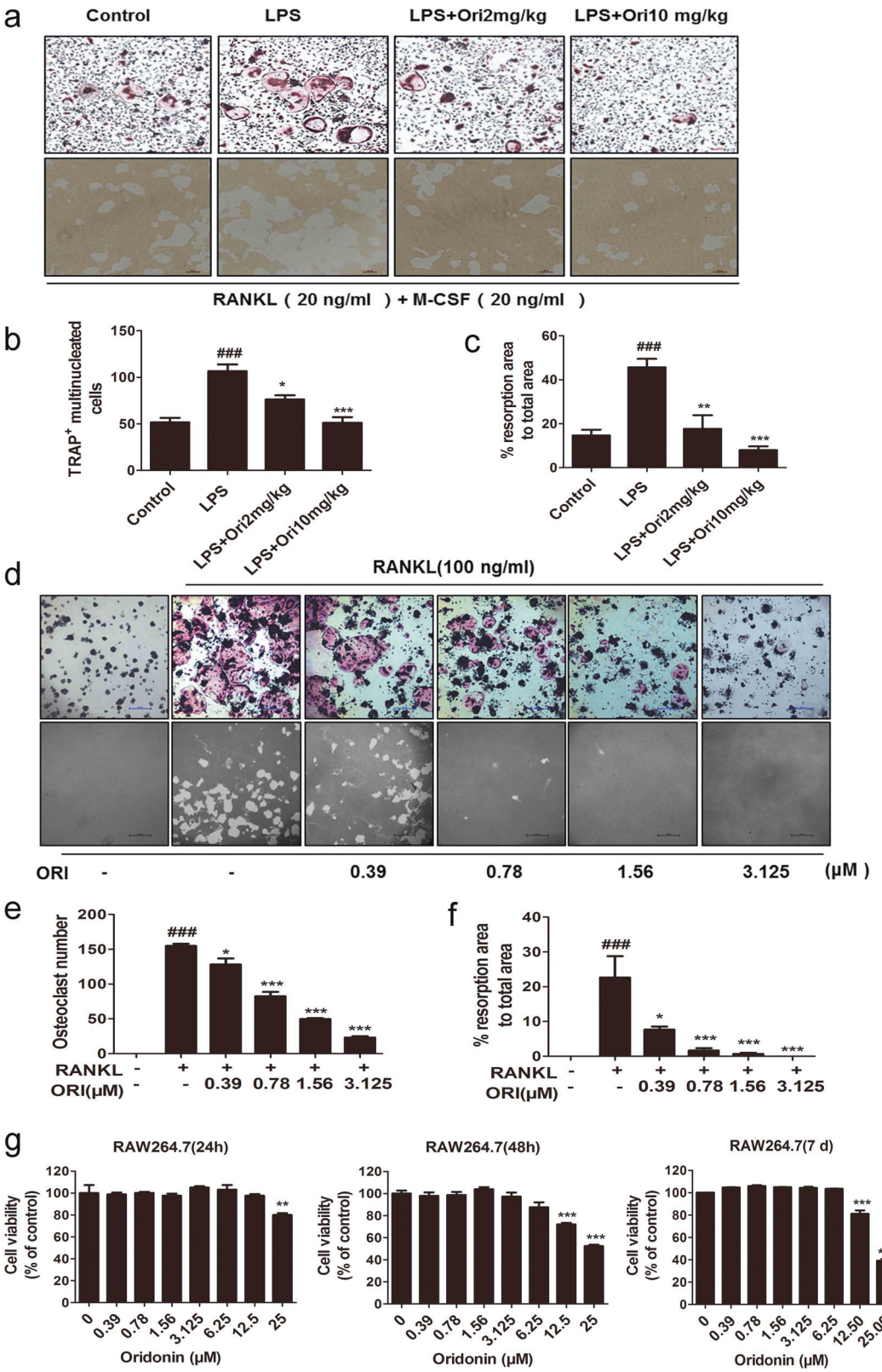

Fig. 2 ORI decreased osteoclast formation and bone resorption in BMMs ex vivo and in RAW264.7 cells in vitro. BMMs from the control group, LPS group, and ORI-treated groups were obtained as described in "Materials and methods" and differentiated into osteoclasts with 20 ng/mL M-CSF and 20 ng/mL RANKL for 3 days for **a**, **b** TRAP staining (scale bars, 100 μm). **a**, **c** Bone resorption pit assays (scale bars, 100 μm). Representative images of **d**, **e** TRAP staining and **d**, **f** resorption pits in RAW264.7 cells were collected (scale bars, 100 μm) and analyzed. **g** Cell viability of RAW264.7 cells after ORI treatment was measured by MTT assays. The results are presented as the mean ± SD of representative experiments. $^{###}P < 0.001$ vs the control group; $^{*}P < 0.05$, $^{**}P < 0.01$, $^{***}P < 0.001$ vs the LPS group.

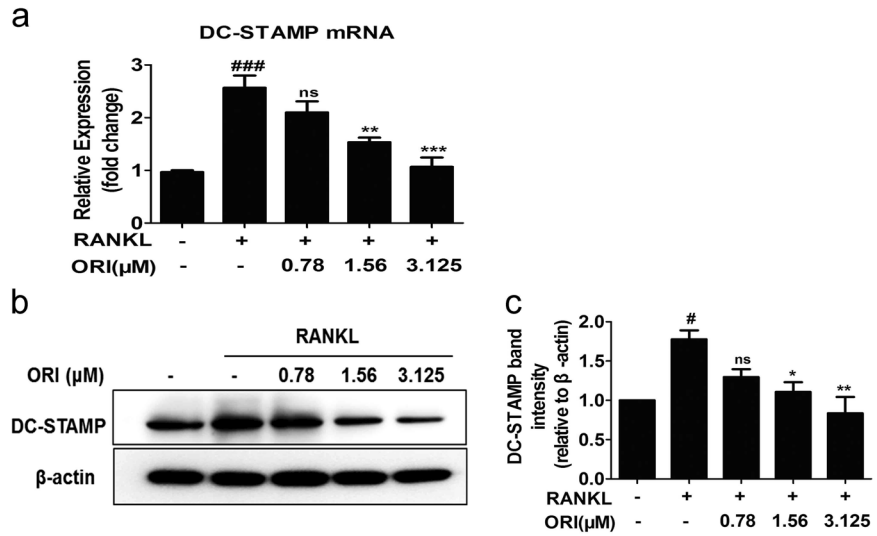

Fig. 3 ORI inhibited RANKL-induced DC-STAMP expression in RAW264.7 cells in vitro. RAW264.7 cells were cultured with RANKL (100 ng/mL) with or without ORI for 24 h, and **a** DC-STAMP mRNA expression was then measured by real-time PCR. RAW264.7 cells were pretreated with or without ORI for 2 h and then stimulated with RANKL (100 ng/mL) for 48 h; **b**, **c** DC-STAMP protein levels were determined by Western blotting. $^{\#}P < 0.05$, $^{\#\#\#}P < 0.001$ vs the control group; $^{*}P < 0.05$, $^{**}P < 0.01$, $^{***}P < 0.001$ vs the RANKL-treated group.

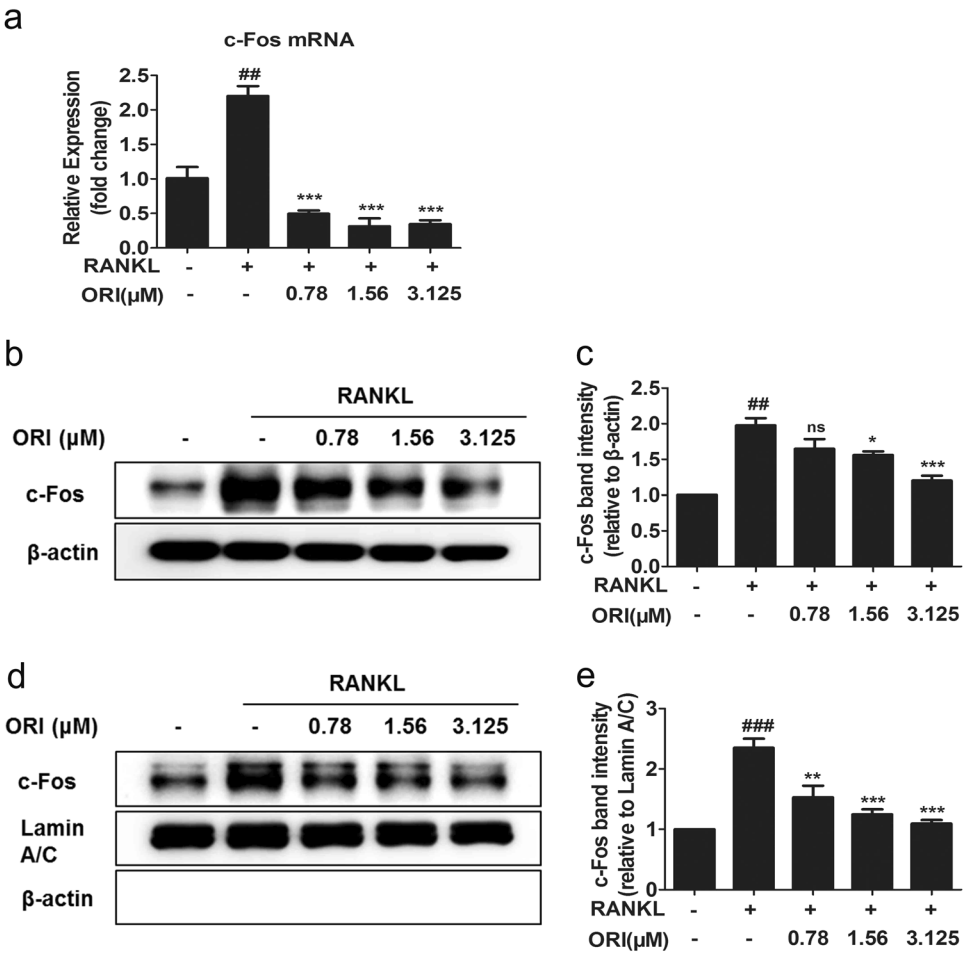

Fig. 4 ORI suppressed the activation of c-Fos in RAW264.7 cells. a RAW264.7 cells were pretreated with or without ORI for 2 h and then stimulated with RANKL (100 ng/mL) for 24 h to examine the mRNA expression of c-Fos. **b**, **c** RAW264.7 cells were induced by RANKL (100 ng/mL) for 30 min to examine the protein expression of c-Fos. **d**, **e** Nuclear extracts from RAW264.7 cells were analyzed by Western blotting with c-Fos, β-actin, and lamin A/C antibodies. $^{\#\#}P < 0.01$, $^{\#\#\#}P < 0.001$ vs the control group; $^{*}P < 0.05$, $^{**}P < 0.01$, $^{***}P < 0.001$ vs the RANKL-treated group.

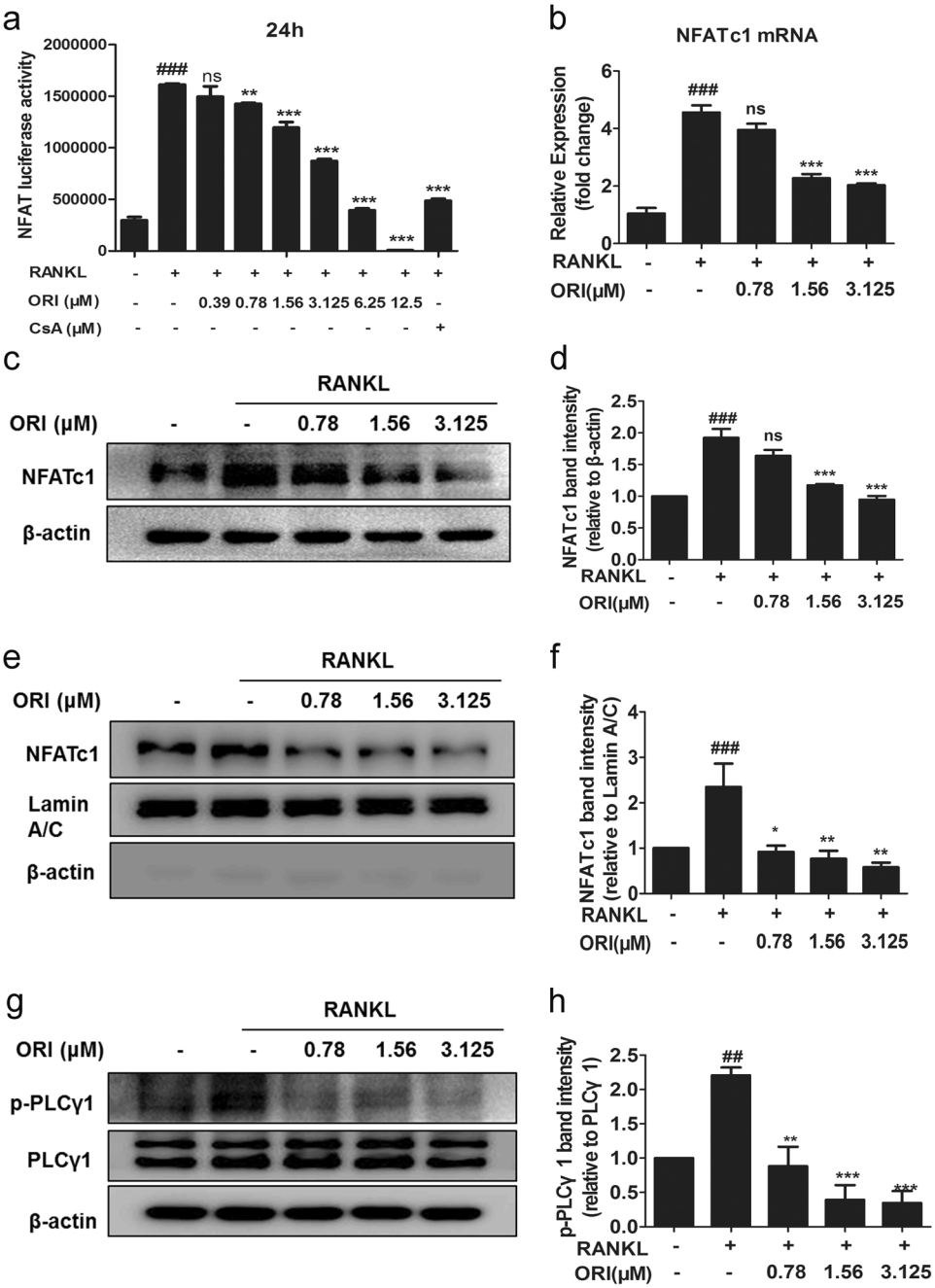

Fig. 5 ORI suppressed the RANKL-induced PLCγ-NFATc1 signaling pathway in RAW264.7 cells. a RAW264.7 cells stably expressing the NFAT-luc luciferase reporter construct were pretreated with ORI and CsA and then stimulated for 24 h with RANKL (100 ng/mL). Then, the luciferase activity was measured. **b** RAW264.7 cells were cultured as described above, and real-time PCR was performed on cells stimulated with or without RANKL and ORI for 24 h to examine NFATc1 mRNA expression. **c–f** Total and nuclear extracts from RAW264.7 cells pretreated with ORI and stimulated with RANKL (100 ng/mL) for 24 h were analyzed by Western blotting with antibodies against NFATc1, lamin A/C, and β-actin. **g**, **h** RAW264.7 cells were pretreated for 30 min with ORI, stimulated with RANKL for 30 min, and analyzed by Western blotting with p-PLCγ1 (Tyr 783), β-actin, and PLCγ1 (1249) antibodies. $^{\#\#}P < 0.01$, $^{\#\#\#}P < 0.001$ vs the control group; $^{*}P < 0.05$, $^{**}P < 0.01$, $^{***}P < 0.001$ vs the RANKL-treated group.

ORI downregulated RANKL-induced osteoclast marker gene expression in RAW264.7 cells

NFATc1 works together with AP-1 in the nucleus to induce the expression of various osteoclast-specific genes [41–43]. Therefore, we examined the expression of osteoclast-specific genes in RAW264.7 cells during osteoclastogenesis. We found that ORI at concentrations from 0.78 to 3.125 μM significantly inhibited the expression of osteoclast-associated genes, including OSCAR, TRAP, c-Src, Fra-2, MMP-9, and cathepsin K, after RANKL stimulation of preosteoclast RAW264.7 cells (Fig. 6).

DC-STAMP-siRNA blocked the inhibitory effects of ORI on NFATc1-luciferase activity and osteoclastogenesis in RAW264.7 cells

We observed that ORI treatment downregulated osteoclastogenesis and the expression of DC-STAMP both in vivo and in vitro. To explore whether ORI acts on osteoclastogenesis by targeting DC-

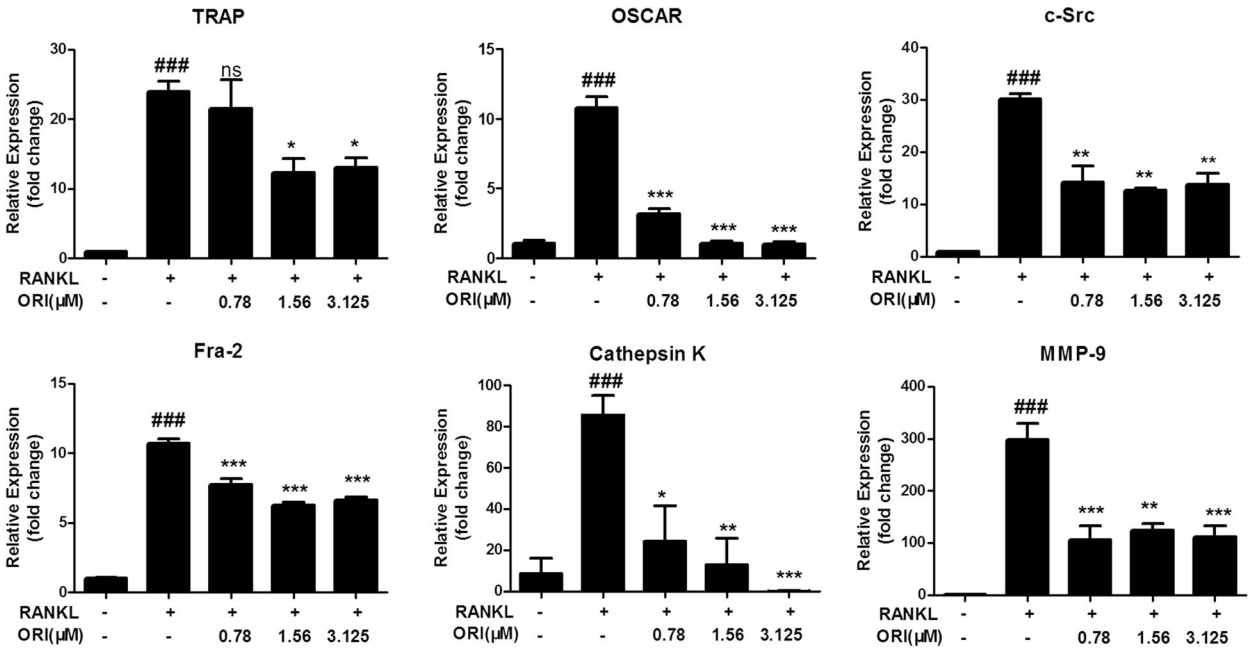

Fig. 6 ORI inhibited RANKL-induced osteoclast marker gene expression in RAW264.7 cells in vitro. RAW264.7 cells were cultured as described above, and qRT-PCR was performed to measure the expression of osteoclast marker genes, including OSCAR, TRAP, c-Src, Fra-2, MMP-9, and cathepsin K. The results are presented as the mean ± SD of representative experiments. $^{###}P < 0.001$ vs the control group; $^{*}P < 0.05$, $^{**}P < 0.01$, $^{***}P < 0.001$ vs the RANKL-treated group.

STAMP, we knocked down DC-STAMP with a specific siRNA in RAW264.7 cells during osteoclastogenesis (Fig. 7a–d). We found that the inhibitory effects of 1.56 μM ORI on osteoclast formation were lost after knockdown of DC-STAMP (Fig. 7e, f). Furthermore, DC-STAMP siRNA decreased the RANKL-induced upregulation of NFATc1-luciferase activity, and the effects of ORI (1.56–3.125 μM) on NFATc1 activity were abrogated after knocking down DC-STAMP (Fig. 7g). These results were consistent with the effect of ORI on osteoclastogenesis, as shown in Fig. 7e. Collectively, these results demonstrated that the inhibition of osteoclast differentiation by ORI was diminished by interfering with DC-STAMP expression. These results further indicate that ORI suppresses osteoclastogenesis by suppressing DC-STAMP expression.

DISCUSSION

Osteoclast differentiation is regarded as a therapeutic target for developing novel drugs to treat bone destruction diseases [2, 8]. Although osteolytic disease treatments aimed at inhibiting osteoclasts, such as anti-RANKL Abs, have been extensively developed during recent decades, oral osteoclast differentiation inhibitors with few side effects are still needed [44–47]. Numerous reports have shown that bone loss is related to inflammatory diseases, in which many prostaglandins and inflammatory cytokines are released [43, 48]. The increased levels of prostaglandins and inflammatory cytokines upregulate the expression of RANKL, which stimulates osteoclast differentiation and function, in multiple cells, such as osteoblasts, activated T cells, synovial fibroblasts, and malignant tumor cells [48, 49]. Here, we observed that ORI could protect against inflammatory bone erosion in vivo and described the mechanism of ORI on osteoclastogenesis.

In LPS-induced inflammatory mice, oral administration of 2 and 10 mg/kg ORI attenuated bone loss and bone erosion in vivo, according to micro-CT and H&E staining results. OSCAR and TRAP mRNA levels were increased in BMMs from model mice. ORI treatment downregulated OSCAR and TRAP mRNA expression and subsequently inhibited osteoclast formation and bone resorption functions ex vivo. Together with ORI-mediated inhibition of RANKL-induced osteoclast differentiation and osteoclast resorption in preosteoclast RAW264.7 cells in vitro, these findings indicate that ORI possesses potential therapeutic effects against inflammatory osteolysis by suppressing osteoclastogenesis.

Interestingly, we observed that DC-STAMP protein expression was increased dramatically in BMMs from LPS-injected mice. Treatment with 2 and 10 mg/kg every day ORI abrogated the upregulation of DC-STAMP expression in preosteoclastic BMMs in comparison with cells from model mice. As DC-STAMP is critical for regulating cell–cell fusion during osteoclastogenesis and because the loss of DC-STAMP results in mature osteoclast deficiency [13, 18, 50], we further explored whether ORI could inhibit osteoclastogenesis by reducing DC-STAMP levels in RAW264.7 cells. As expected, RANKL upregulated DC-STAMP expression. ORI administration inhibited both the mRNA and protein expression of DC-STAMP in RAW264.7 cells during RANKL-induced osteoclastogenesis in vitro.

DC-STAMP-knockdown reduces Ca^{2+}-NFATc1 signaling during osteoclastogenesis [19]. NFATc1-deficient osteoclast precursors fail to differentiate into osteoclasts but can efficiently form osteoclasts after NFATc1 overexpression, even in the absence of RANKL [5, 41]. NFATc1-deficient mice exhibit an osteopetrotic phenotype due to a severe defect in osteoclast formation [4, 41]. NFATc1 is a master regulator of osteoclastogenesis and bone absorption functions [11]. In the present study, cytoplasmic and nuclear NFATc1 expression and NFAT-luciferase activity were strongly inhibited by ORI in RAW264.7 cells during RANKL-induced osteoclastogenesis. In addition, PLCγ1 phosphorylation, which can initiate the activation and nuclear translocation of NFATc1 [33], was downregulated by ORI in RANKL-induced osteoclast differentiation in vitro. The reduced PLCγ1 and NFATc1 activation were consistent with the decreased DC-STAMP expression in RAW264.7 cells after RANKL stimulation.

c-Fos, a component of the AP-1 complex, is activated by RANKL and required for NFATc1 expression during osteoclastogenesis [41–43]. c-Fos-deficient mice displayed reduced NFATc1 expression and an osteopetrotic bone phenotype [4, 41, 51]. Here, we found that the mRNA expression of c-Fos was drastically

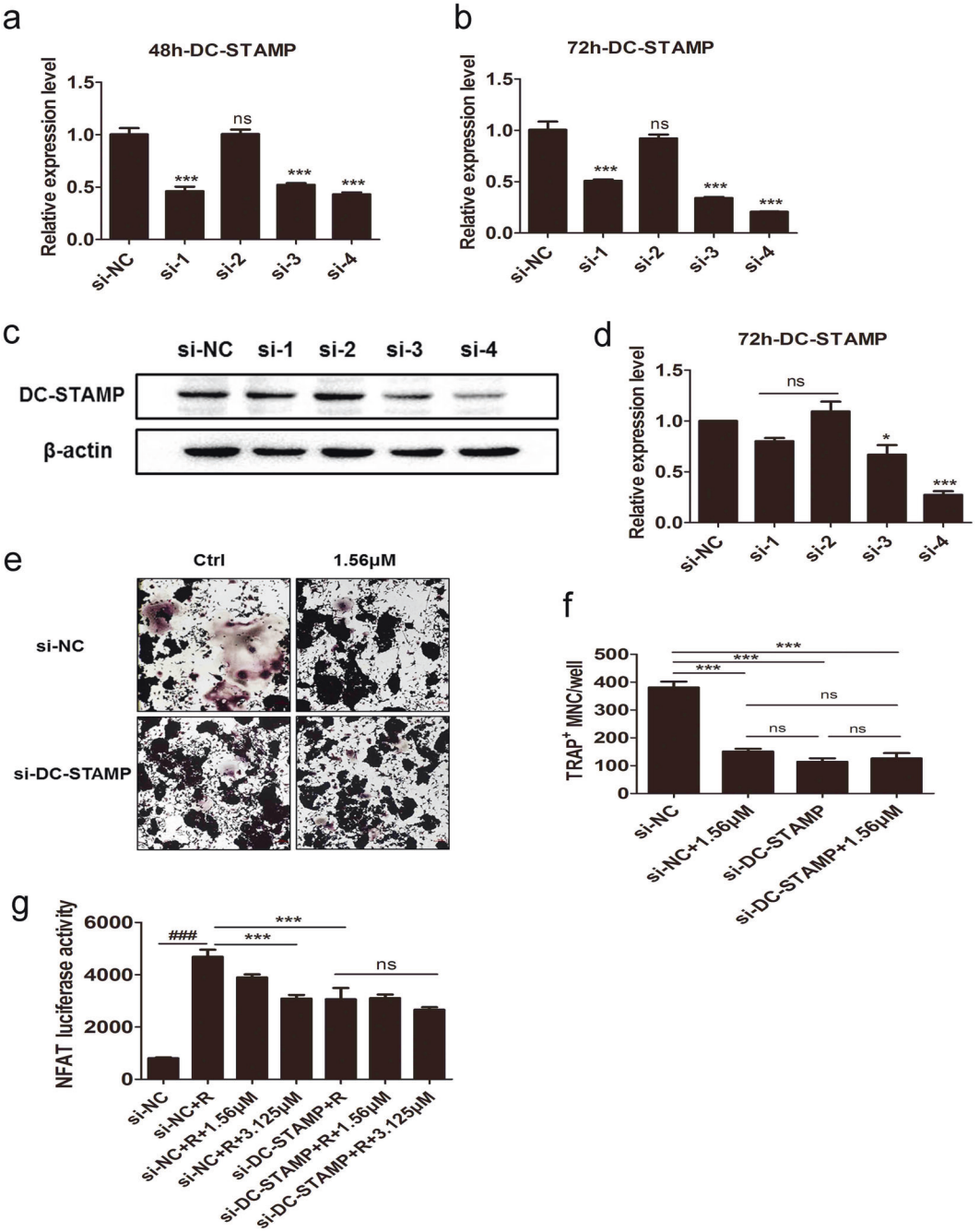

Fig. 7 DC-STAMP-siRNA abolished the inhibitory effects of ORI on osteoclast formation and NFATc1 expression. We synthesized four target siRNA sequences and verified their knockdown efficiency by **a**, **b** qPCR and **c**, **d** WB; the siRNA with the highest knockout efficiency was used for the follow-up experiments. **e** RAW264.7 cells were seeded and transfected with siRNA-DC-STAMP (40 nM) using Lipofectamine RNAIMAX. After ~24 h of siRNA interference, the cells were stimulated by RANKL with or without ORI (1.56 μM). The media were changed every 2 days. After 4 days, the cells were stained with TRAP. **f** $TRAP^{+}$ multinucleated cells (>3 nuclei) were counted as mature OCs. **g** RAW264.7 cells stably expressing the NFAT-luc luciferase reporter construct were transfected with siRNA-DC-STAMP for 24 h and then treated with ORI (1.56–3.125 μM) and RANKL (100 ng/mL) for 24 h. The luciferase activity was measured to indicate NFATc1 transcription. **a**–**f** $^{*}P < 0.05$, $^{***}P < 0.001$ vs the si-NC group. **g** $^{\#\#\#}P < 0.001$ vs the si-NC group; $^{*}P < 0.05$, $^{***}P < 0.001$ vs the RANKL-treated group.

attenuated after ORI treatment in RANKL-stimulated RAW264.7 cells in vitro. In addition, suppression of the nuclear expression of c-Fos by ORI was observed in RAW264.7 cells during osteoclastogenesis.

Nuclear NFATc1 can bind to DNA and directly induce the expression of osteoclast-related genes in cooperation with c-Fos [52–54]. Consistent with the decreased protein levels of nuclear c-Fos and NFATc1, ORI inhibited the expression of osteoclast-related genes, including Cathepsin K, c-Src, MMP-9, TRAP, OSCAR, and Fra-2, in RANKL-stimulated preosteoclast RAW264.7 cells, which contributed to osteoclastogenesis and bone absorption in vitro.

These results showed that ORI decreased DC-STAMP expression and downstream factors, including c-Fos and NFATc1, when suppressing osteoclastogenesis. We further evaluated whether ORI exerted inhibitory effects on osteoclastogenesis by targeting DC-STAMP. We knocked down DC-STAMP expression in RAW264.7

cells during osteoclastogenesis using DC-STAMP siRNA. Notably, after knocking down DC-STAMP, ORI exhibited no suppressive effects on osteoclastogenesis; in addition, ORI showed no obvious inhibition of NFATc1-luciferase activity after RANKL stimulation in NFAT-luc-RAW264.7 cells, which suggested that ORI-mediated inhibition of NFATc1 activity during osteoclastogenesis was also abolished after knocking down DC-STAMP by siRNA. These observations further demonstrate that ORI can inhibit osteoclast differentiation through DC-STAMP.

In summary, we demonstrated that DC-STAMP expression was increased in mice with LPS-induced bone loss, and oral ORI attenuated inflammation-induced osteolysis in vivo by reducing DC-STAMP expression. Our data also suggest that ORI suppresses osteoclastogenesis via a new mechanism, suppressing DC-STAMP expression and subsequently decreasing the downstream c-Fos and PLCγ-NFATc1 signaling pathways. Thus, ORI is a potential treatment for osteoclast-related inflammatory osteolytic diseases, such as psoriatic arthritis, rheumatoid arthritis, and periodontitis, by suppressing DC-STAMP. Recently, it has been reported that ORI is an NLRP3 inhibitor with strong anti-inflammatory activity [32], but there has been no report to address the relationship between NLRP3 and osteoclasts. Our data provide a novel pathway by which ORI can be used to treat bone loss diseases with osteoclast overactivation through modulating DC-STAMP. The therapeutic effects and mechanisms of ORI on DC-STAMP-mediated bone diseases in humans deserve further exploration.

ACKNOWLEDGEMENTS

This work was supported by Guangzhou Science and Technology Plan Project (201804010027) and the National Natural Science Foundation of China (81773740, 81073119).

AUTHOR CONTRIBUTIONS

Study conception and design: BHZ and XJL. Acquisition, analysis, and interpretation of data: BHZ, YHT, WDD, JHZ, QY, ZBD, and MHK. Drafting/revision of the work for intellectual content and context: BHZ and XJL. Final approval and overall responsibility for the published work: XJL.

ADDITIONAL INFORMATION

Competing interests: The authors declare no competing interests.

REFERENCES

1. Helming L, Gordon S. Molecular mediators of macrophage fusion. Trends Cell Biol. 2009;19:514–22.
2. Ono T, Nakashima T. Recent advances in osteoclast biology. Histochem Cell Biol. 2018;149:325–41.
3. Hirotani H, Tuohy NA, Woo JT, Stern PH, Clipstone NA. The calcineurin/nuclear factor of activated T cells signaling pathway regulates osteoclastogenesis in RAW264.7 cells. J Biol Chem. 2004;279:13984–92.
4. Matsuo K, Galson DL, Zhao C, Peng L, Laplace C, Wang KZ, et al. Nuclear factor of activated T-cells (NFAT) rescues osteoclastogenesis in precursors lacking c-Fos. J Biol Chem. 2004;279:26475–80.
5. Ikeda F, Nishimura R, Matsubara T, Hata K, Reddy SV, Yoneda T. Activation of NFAT signal in vivo leads to osteopenia associated with increased osteoclastogenesis and bone-resorbing activity. J Immunol. 2006;177:2384–90.
6. Takayanagi H. The role of NFAT in osteoclast formation. Ann N Y Acad Sci. 2007;1116:227–37.
7. Fechtenbaum J, Cropet C, Kolta S, Horlait S, Orcel P, Roux C. The severity of vertebral fractures and health-related quality of life in osteoporotic postmenopausal women. Osteoporos Int. 2005;16:2175–9.
8. Boyce BF. Advances in osteoclast biology reveal potential new drug targets and new roles for osteoclasts. J Bone Miner Res. 2013;28:711–22.
9. Li T, Wu SM, Xu ZY, Ou-Yang S. Rabbiteye blueberry prevents osteoporosis in ovariectomized rats. J Orthop Surg Res. 2014;9:56.
10. Cauley JA. Osteoporosis: fracture epidemiology update 2016. Curr Opin Rheumatol. 2017;29:150–6.
11. Negishi-Koga T, Takayanagi H. Ca^{2+}-NFATc1 signaling is an essential axis of osteoclast differentiation. Immunol Rev. 2009;231:241–56.
12. Kim J, Yang J, Park OJ, Kang SS, Kim WS, Kurokawa K, et al. Lipoproteins are an important bacterial component responsible for bone destruction through the induction of osteoclast differentiation and activation. J Bone Miner Res. 2013;28:2381–91.
13. Yagi M, Miyamoto T, Sawatani Y, Iwamoto K, Hosogane N, Fujita N, et al. DC-STAMP is essential for cell-cell fusion in osteoclasts and foreign body giant cells. J Exp Med. 2005;202:345–51.
14. Miyamoto T. The dendritic cell-specific transmembrane protein DC-STAMP is essential for osteoclast fusion and osteoclast bone-resorbing activity. Mod Rheumatol. 2006;16:341–2.
15. Chiu YH, Mensah KA, Schwarz EM, Ju Y, Takahata M, Feng C, et al. Regulation of human osteoclast development by dendritic cell-specific transmembrane protein (DC-STAMP). J Bone Miner Res. 2012;27:79–92.
16. Kukita T, Wada N, Kukita A, Kakimoto T, Sandra F, Toh K, et al. RANKL-induced DC-STAMP is essential for osteoclastogenesis. J Exp Med. 2004;200:941–6.
17. Baek JM, Kim JY, Jung Y, Moon SH, Choi MK, Kim SH, et al. Mollugin from Rubea cordifolia suppresses receptor activator of nuclear factor-kappaB ligand-induced osteoclastogenesis and bone resorbing activity in vitro and prevents lipopolysaccharide-induced bone loss in vivo. Phytomedicine. 2015;22:27–35.
18. Chiu YH, Ritchlin CT. DC-STAMP: a key regulator in osteoclast differentiation. J Cell Physiol. 2016;231:2402–7.
19. Chiu YH, Schwarz E, Li D, Xu Y, Sheu TR, Li J, et al. Dendritic cell-specific transmembrane protein (DC-STAMP) regulates osteoclast differentiation via the Ca^{2+} /NFATc1 Axis. J Cell Physiol. 2017;232:2538–49.
20. Iwasaki R, Ninomiya K, Miyamoto K, Suzuki T, Sato Y, Kawana H, et al. Cell fusion in osteoclasts plays a critical role in controlling bone mass and osteoblastic activity. Biochem Biophys Res Commun. 2008;377:899–904.
21. Wisitrasameewong W, Kajiya M, Movila A, Rittling S, Ishii T, Suzuki M, et al. DC-STAMP is an osteoclast fusogen engaged in periodontal bone resorption. J Dent Res. 2017;96:685–93.
22. Chiu YG, Ritchlin CT. Characterization of DC-$STAMP^{+}$ cells in human bone marrow. J Bone Marrow Res. 2013;1:1000127. https://doi.org/10.4172/2329-8820.1000127.
23. Owona BA, Schluesener HJ. Molecular insight in the multifunctional effects of oridonin. Drugs R D. 2015;15:233–44.
24. Ren CM, Li Y, Chen QZ, Zeng YH, Shao Y, Wu QX, et al. Oridonin inhibits the proliferation of human colon cancer cells by upregulating BMP7 to activate p38 MAPK. Oncol Rep. 2016;35:2691–8.
25. Rajkumar T, Yamuna M. Multiple pathways are involved in drug resistance to doxorubicin in an osteosarcoma cell line. Anticancer Drugs. 2008;19:257–65.
26. Xu ZZ, Fu WB, Jin Z, Guo P, Wang WF, Li JM. Reactive oxygen species mediate oridonin-induced apoptosis through DNA damage response and activation of JNK pathway in diffuse large B cell lymphoma. Leuk Lymphoma. 2016;57:888–98.
27. Wang S, Zhong Z, Wan J, Tan W, Wu G, Chen M, et al. Oridonin induces apoptosis, inhibits migration and invasion on highly-metastatic human breast cancer cells. Am J Chin Med. 2013;41:177–96.
28. Lu Y, Sun Y, Zhu J, Yu L, Jiang X, Zhang J, et al. Oridonin exerts anticancer effect on osteosarcoma by activating PPAR-gamma and inhibiting Nrf2 pathway. Cell Death Dis. 2018;9:15.
29. Li FF, Yi S, Wen L, He J, Yang LJ, Zhao J, et al. Oridonin induces NPM mutant protein translocation and apoptosis in $NPM1c^{+}$ acute myeloid leukemia cells in vitro. Acta Pharmacol Sin. 2014;35:806–13.
30. Xie Z, Yu H, Sun X, Tang P, Jie Z, Chen S, et al. A novel diterpenoid suppresses osteoclastogenesis and promotes osteogenesis by inhibiting lfrd1-mediated and IkappaBalpha-mediated p65 nuclear translocation. J Bone Miner Res. 2018;33:667–78.
31. Viniegra A, Goldberg H, Cil C, Fine N, Sheikh Z, Galli M, et al. Resolving macrophages counter osteolysis by anabolic actions on bone cells. J Dent Res. 2018;97:1160–9.
32. He H, Jiang H, Chen Y, Ye J, Wang A, Wang C, et al. Oridonin is a covalent NLRP3 inhibitor with strong anti-inflammasome activity. Nat Commun. 2018;9:2550.
33. Zeng X, Zhang Y, Wang S, Wang K, Tao L, Zou M, et al. Artesunate suppresses RANKL-induced osteoclastogenesis through inhibition of PLCgamma1-Ca^{2+}-NFATc1 signaling pathway and prevents ovariectomy-induced bone loss. Biochem Pharmacol. 2017;124:57–68.
34. Zhou L, Liu Q, Yang M, Wang T, Yao J, Cheng J, et al. Dihydroartemisinin, an antimalaria drug, suppresses estrogen deficiency-induced osteoporosis, osteoclast formation, and RANKL-induced signaling pathways. J Bone Miner Res. 2016;31:964–74.
35. Kwak HB, Lee BK, Oh J, Yeon JT, Choi SW, Cho HJ, et al. Inhibition of osteoclast differentiation and bone resorption by rotenone, through down-regulation of RANKL-induced c-Fos and NFATc1 expression. Bone. 2010;46:724–31.

36. Lee JM, Park H, Noh AL, Kang JH, Chen L, Zheng T, et al. 5-Lipoxygenase mediates RANKL-induced osteoclast formation via the cysteinyl leukotriene receptor 1. J Immunol. 2012;189:5284–92.
37. Zhai ZJ, Li HW, Liu GW, Qu XH, Tian B, Yan W, et al. Andrographolide suppresses RANKL-induced osteoclastogenesis in vitro and prevents inflammatory bone loss in vivo. Br J Pharmacol. 2014;171:663–75.
38. Park HJ, Son HJ, Sul OJ, Suh JH, Choi HS. 4-Phenylbutyric acid protects against lipopolysaccharide-induced bone loss by modulating autophagy in osteoclasts. Biochem Pharmacol. 2018;151:9–17.
39. Yin Y, Tang L, Chen J, Lu X. MiR-30a attenuates osteoclastogenesis via targeting DC-STAMP-c-Fos-NFATc1 signaling. Am J Transl Res. 2017;9:5743–53.
40. Dou C, Zhang C, Kang F, Yang X, Jiang H, Bai Y, et al. MiR-7b directly targets DC-STAMP causing suppression of NFATc1 and c-Fos signaling during osteoclast fusion and differentiation. Biochim Biophys Acta. 2014;1839:1084–96.
41. Takayanagi H, Kim S, Koga T, Nishina H, Isshiki M, Yoshida H, et al. Induction and activation of the transcription factor NFATc1 (NFAT2) integrate RANKL signaling in terminal differentiation of osteoclasts. Dev Cell. 2002;3:889–901.
42. Asagiri M, Sato K, Usami T, Ochi S, Nishina H, Yoshida H, et al. Autoamplification of NFATc1 expression determines its essential role in bone homeostasis. J Exp Med. 2005;202:1261–9.
43. Takayanagi H. Osteoimmunology: shared mechanisms and crosstalk between the immune and bone systems. Nat Rev Immunol. 2007;7:292–304.
44. Kennel KA, Drake MT. Adverse effects of bisphosphonates: implications for osteoporosis management. Mayo Clin Proc. 2009;84:632–7. quiz 8
45. Andrews EB, Gilsenan AW, Midkiff K, Sherrill B, Wu Y, Mann BH, et al. The US postmarketing surveillance study of adult osteosarcoma and teriparatide: study design and findings from the first 7 years. J Bone Miner Res. 2012;27:2429–37.
46. Huang Z, Ding C, Li T, Yu SP. Current status and future prospects for disease modification in osteoarthritis. Rheumatology. 2018;57:iv108–23.
47. Compston JE, McClung MR, Leslie WD. Osteoporosis. Lancet. 2019;393:364–76.
48. Danks L, Takayanagi H. Immunology and bone. J Biochem. 2013;154:29–39.
49. Fadda S, Hamdy A, Abulkhair E, Mahmoud Elsify H, Mostafa A. Serum levels of osteoprotegerin and RANKL in patients with rheumatoid arthritis and their relation to bone mineral density and disease activity. Egypt Rheumatologist. 2015;37:1–6.
50. Zeng Z, Zhang C, Chen J. Lentivirus-mediated RNA interference of DC-STAMP expression inhibits the fusion and resorptive activity of human osteoclasts. J Bone Miner Metab. 2013;31:409–16.
51. Grigoriadis AE, Wang ZQ, Cecchini MG, Hofstetter W, Felix R, Fleisch HA, et al. c-Fos: a key regulator of osteoclast-macrophage lineage determination and bone remodeling. Science. 1994;266:443–8.
52. Wada T, Nakashima T, Hiroshi N, Penninger JM. RANKL-RANK signaling in osteoclastogenesis and bone disease. Trends Mol Med. 2006;12:17–25.
53. Nakashima T, Takayanagi H. New regulation mechanisms of osteoclast differentiation. Ann N Y Acad Sci. 2011;1240:E13–8.
54. Park JH, Lee NK, Lee SY. Current understanding of RANK signaling in osteoclast differentiation and maturation. Mol Cells. 2017;40:706–13.